Bidirectional optoantenna for radio over fiber architectures

José María Cela París and Damià Casas Casajuana
Universitat Politècnica de Catalunya, Barcelona, Spain
(Dated: June 5, 2021)

Abstract: This paper proposes an innovative optoantena design, result of the combination of a laser and photodiode for fiber transmission and reception with a dual port full-duplex antenna. This antenna can operate at different frequency bands simultaneously, while keeping it's two ports highly isolated. Moreover the antenna combines filtering, duplexing and radiating thus reducing cost, volume and weight when compared to a more traditional approach. This properties make this design a perfect candidate for the implementation of radio over fiber techniques. Both the design of the antenna and the characterization of the optoelectronic elements of the device are thoroughly discussed in this paper.

I. INTRODUCTION

The present evolution of the communications and remote sensing markets, allows to predict that only through the Smart combination of wireless and fiber optics technologies can the demand for seamless coverage, low-loss transmission and wide bandwidth be satisfied [1]. The design of compact, low cost volume and weight wireless terminals that may connect directly to fiber is expected to play a key role towards the next systems generation. That explains the recent popularity growth of *Radio over fiber* (RFoF) techniques in which the wireless signal is transmitted in native format through fiber so the wireless nodes can be kept simple and transparently bridge the radiofrequency envelope in between the optical and the wireless domains

A device that encompasses such characteristics can play a big role in the upcoming internet of things (IoT) technology. This technology has many promising applications, but at the same time several technical challenges arise. Some of these obstacles are spectrum saturation and attenuation of signals at high frequencies. In the present paper, we present a solution to solve these problems with the design of a dual-band optoantenna for for the full-duplex fiber-radio connection. The LTE 22 band with a FDD duplex mode has been targeted for this design.

II. DEVICE STRUCTURE

The device can be divided in two parts: the optoelectronic circuitry and the antenna.

The main electronic parts of the optoelectronic circuit are the low-cost Transmitter/Receiver Optical SubAssembly (TOSA/ROSA) units. The TOSA consists on a distributed feedback (DFB) transmitter laser with emission band centered at $l = 1.3\mu m$. And the ROSA, which includes a PIN photodiode receiver connected to a transimpedance (TIA) amplifier. Their main function is to convert the received optical signal into an electric signal and vice versa. The circuitry also accomplishes DC feeding requirements and impedance matching with the antenna.

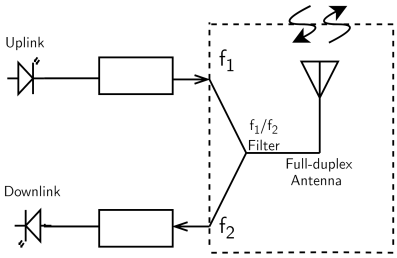

FIG. 1: Diagram of the proposed full-duplex device

The antenna consists of a two-port aperture-fed patch to radiate and receive the RF signal and a filter. The filter is made of various resonators. These resonators are responsible of separating the uplink and downlink frequencies, in order to deliver two different signals to the circuitry. Furthermore, this antenna has the capability of operating at both frequencies while keeping both ports isolated.

III. ELECTRONIC COMPONENTS

The chosen components are the FP-1310-4I laser and the PIN-1310-10LR-LC photodiode. Those are off-the-shelf (OTS) cost-effective components easily integrable with the proposed structure and the optical backend.

In the laser side, DC power and signal are delivered superposed in the same input pin. The current coming from the power supply is regulated using three 20Ω resistances. Three resistances were used instead of one, in order to be within the power ratings, and to have a better control of the current flow. Additionally an inductance of 100nH was used to not let RF signal into the power supply.

As mentioned before, the package of the photodiode includes an amplifier inside of it, which is fed with the same DC input as the laser. Unlike the laser, power and signal go through different pins, but we also used an inductance (100nH) to protect the power supply in case it exists some coupling. Both photodiode and laser work

at the wavelength of 1310 nm and support bit rates up to 10Gb/s.

A. Characterization

The characterization and modeling of the two components is necessary to isolate their real frequency response from the rest of testing circuit, like transmission lines and welds (de-embedding). The first objective is to find a lumped element model of the components. Afterwards, a matching network is proposed to adapt the circuit and antenna impedances. The modeling of the components is made using the Keysight Advanced Design System (ADS) software. The laser model follows the circuit proposed by M. S. Ozyazici [2]. Although, the scheme was simplified because our measures did present negligible losses.

With the purpose of making the initial measurements a testing microstrip board is printed to fit our model. We used FR4 as the substrate and copper coattings ($\sigma_{CU} = 5.96 \cdot 10^7 S/m$) of $35\mu m$. The laser, the photodiode and the basic components are included in the prototype.

The frequency response of the components is obtained using a vector network analyzer (VNA). The VNA returns S-parameter measurements at various frequencies. The measurements are performed between 3 and 4 GHz as this spectrum band was targeted. The equivalent input impedance is obtained with single-port independent measurements of the laser and the photodiode. The signal transmission between both elements is also tested through an optical fiber. The S21 parameter shows a -20 dB gain from both ends, mainly due to the mismatch between the ports and the impedance of the laser and the photodiode.

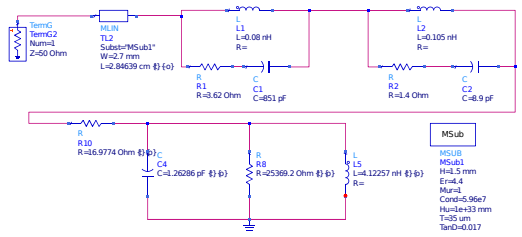

FIG. 2: Photodiode modeling on ADS

A flat zone with low loses was observed near 3.5GHz. Thereby, the LTE 22 band is proven a good choice for this design.

The S-parameters of the model are fitted to those measured, by tunning the values of the lumped components. Then, when a good starting point is reached, one can use the optimizing algorithms of the ADS software. Using an error function with the difference between simulated and real responses, the software provides the best values of the lumped elements of the model. In practice, several optimization algorithms were used. Most useful ones

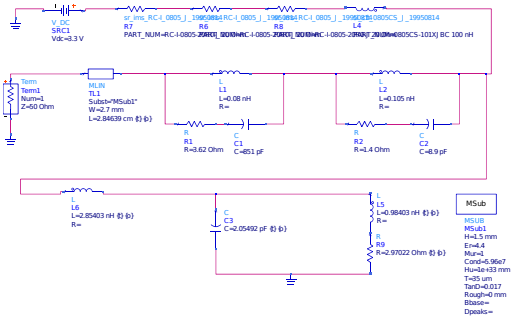

FIG. 3: Laser diode modeling on ADS

for this task are the gradient and simulated annealing algorithms. The results of the fitting are presented on a Smith chart in Fig. 4 and 5.

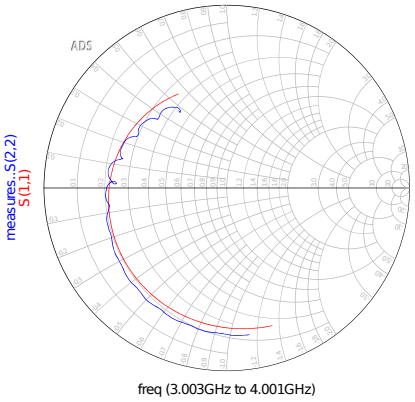

FIG. 4: Photodiode real measures in front of characterization.

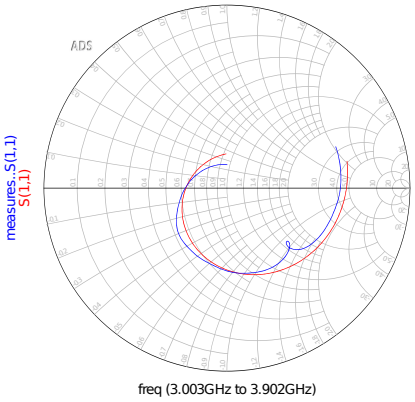

FIG. 5: Laser real measures in front of characterization.

IV. IMPEDANCE MATCHING

Finally, a circuit to match the impedance of the antenna is designed with the help of ADS software. We

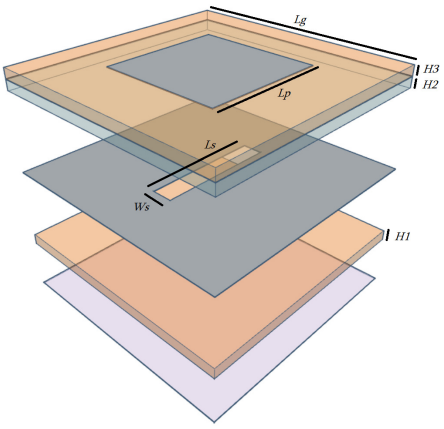

FIG. 6: Vertical dissection of the antenna. Bottom layer contains the resonators

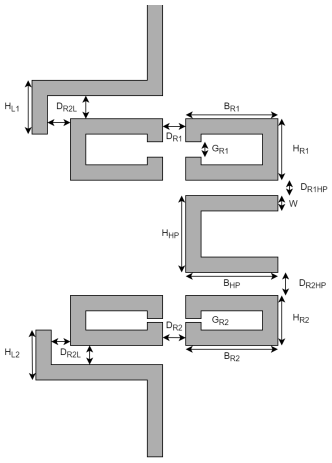

FIG. 7: Resonator diagram

decided to match both the antenna and the RF circuitry to 50 Ohms. This way, the optoantenna design can be adapted to different requirements by changing only the antenna part. Thanks to the de-embedding, we were able to match the response of the circuit without the extra transmission lines of the test board and DC-blocks. The impedance matching is carried out with a transmission line and an open stub, since a narrowband operation is enough for the current solution.. The electrical length of each component is such that the impedance matching is maximized at the center uplink/downlink frequency.

V. ANTENNA DESIGN AND SIMULATION

The antenna is designed and simulated using the software CST Studio Suite.

The design of the antenna is based on the one proposed in [3]. This design makes use of open loop and hairpin resonators to implement the desired filters. The structure of the antenna is shown in Fig. 6 is made of two Rogers RO4003C substrates represented by the orange pieces. Between the substrates a small permittivity foam (blue piece in Fig6) is placed to separate them. A square patch is printed on the top layer of the upper substrate and a conductor plane with a slot is printed on the entirety the top layer of the lower substrate. Finally, the feeding lines and the resonators (purple surface in Fig.6) are printed the bottom layer of the lower substrate.

The filtering of the two channels is accomplished by two open loop resonator pairs, each with a different resonant frequency, $f_1 = 3.4$GHz for the top one, acting as uplink, and $f_2 = 3.6$GHz for the lower one, acting as downlink. The two pairs of resonators are coupled to the hairpin resonator in between them, this hairpin resonator is tuned to a central frequency f_0, which is shared by the patch. The conductor plane printed on top of the lower substrate acts as a common ground for both the patch and the resonators, as well as for the feeding lines. This conductor plane also helps to reduce the interference between the radiation of the patch and the resonator network. However a small slot is left uncovered in this plane, to allow the coupling of the hairpin resonator and the patch.

To design the resonators, we make use of the fact that this resonators select a wavelength approximately equal to their total length, in other words:

$$L_T \approx \frac{\lambda}{2} \tag{1}$$

Where L_T represents the total length of the resonator (both open-loop and hairpin). If we translate this result to frequency, we get the following rule to design a resonator at frequency f:

$$L_T \approx \frac{c}{2f\sqrt{\varepsilon_r}} \tag{2}$$

In the case of our material of choice, Rogers RO4003C, it's relative permittivity is $\varepsilon_r = 3.55$. Expression 2 is a good starting point, but a finer tuning is required to really select the desired frequency. Additionally the width of the microstrip lines is calculated in order to get a characteristic impedance $Z_0 = 50\Omega$.

The simulation of the antenna behavior and the use of the optimizing tools allows us to choose the set of geometrical parameters that result in the desired performance. The numeric values of this parameters are contained in Table I and represented in figures 6 and 7

H_{HP}	B_{HP}	B_{R1}	H_{R1}	G_{R1}	D_{R1}	D_{R1L}	D_{R1HP}	
9.74	9.20	9.20	7.42	0.60	0.50	0.40	0.40	
Lg	Lp	B_{R2}	H_{R2}	G_{R2}	D_{R2}	D_{R2L}	D_{R1HP}	
90.0	28.0	9.20	5.60	0.60	0.51	0.40	0.4	
W	H_1	H_2	H_3	W_S	L_S	D_S	H_{L1}	H_{L2}
1.13	0.50	2.50	1.0	2.02	19.83	5.00	1.0	1.0

TABLE I: Antenna Dimensions (mm)

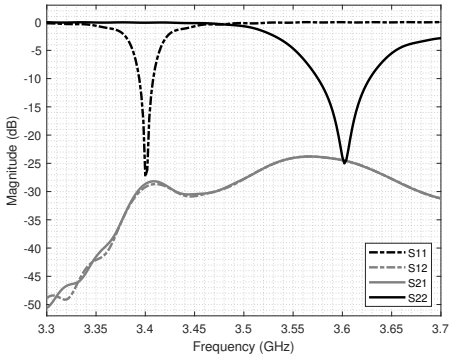

FIG. 8: S-parameters of the antenna

The parameter D_S needs some clarification, since it is the deviation of the slot from the centre of the ground plane, along the slot's long axis.

With this values, the whole antenna was simulated. And the S-parameters obtained are those seen in Fig. 8. It can be observed that both $S(1,1)$ and $S(2,2)$ are well below -20dB at their respective frequencies. This ensures a very low reflection coefficient in both ports 1 and 2, and thus a maximum power transfer when operating at their respective frequencies. Moreover, $S(1,2)$ and $S(2,1)$, are both quite low, at around -30dB for the whole frequency range, and therefore a good isolation between ports is guaranteed. It is clear that uplink channel has a smaller bandwidth than the downlink one. More precisely, the bandwidth computed at -10dB is:

$$FBW_1 = \frac{3.408 - 3.394}{3.4} = 0.4118\% \tag{3}$$

$$FBW_2 = \frac{3.628 - 3.576}{3.6} = 1.4444\% \tag{4}$$

The radiating behaviour of the antenna is presented in Fig. 9 and 10. In these figures the direction of the Z axis goes from the patch towards the resonator. Therefore the angle $\theta = 180^{\text{o}}$ is aligned with the patch, and so, the main lobe is also aligned with it. Hence the antenna radiates mainly from the patch, and quite less from the resonators.

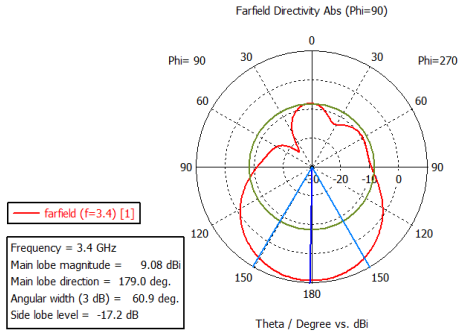

FIG. 9: Farfield directivity at $f_1 = 3.4$GHz, port 1 excited

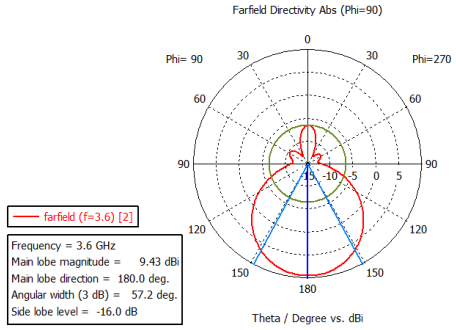

FIG. 10: Farfield directivity at $f_2 = 3.6$GHz, port 2 excited

VI. CONCLUSION

This paper has demonstrated the use of an optoantena like the one proposed as an effective solution for radio over fiber bidirectional communications. Their low cost, reduced size and good performance makes designs like this one strong contenders for future applications specially in the field of IoT.

However this design has only been tested from a simulation standpoint, and is still lacking experimental evidence to support it. In the near future the whole system should be printed and tested to see if measured data agrees with the simulations. If so, the validity of this design would be reaffirmed.

[1] Francisco Aznar Concepción Aldea Diego F. Paredes-Páliz, Guillermo Royo and Santiago Celma. Radio over fiber: An alternative broadband network technology for iot. *Electronics*, 9:1785–1791, 2020.

[2] M. S. Ozyazici. The complete electrical equivalent circuit of a double heterojunction laser diode using scatterring parameters. *Journal of Optoelectronics and Advanced Materials*, 6(4):1243 – 1253, 2004.

[3] Chun-Xu Mao, Steven Gao, and Yi Wang. Dual-band full-duplex tx/rx antennas for vehicular communications. *IEEE Transactions on Vehicular Technology*, 67(5):4059–4070, 2018.